

NUMERICAL FLOW ANALYSIS OF THE ISS RE-ENTRY

F. Zander⁽¹⁾, S. Löhle⁽¹⁾, H. Krag⁽²⁾, S. Lemmens⁽²⁾, R. J. Gollan⁽³⁾, and P. A. Jacobs⁽³⁾

⁽¹⁾*High Enthalpy Flow Diagnostics Group, Institute for Space Systems, University of Stuttgart, Stuttgart, Germany, Email: {zander, loehle}@irs.uni-stuttgart.de*

⁽²⁾*Space Debris Office, ESA/ESOC, Darmstadt, Germany, Email: {Holgar.Krag, Stijn.Lemmens}@esa.int*

⁽³⁾*Centre for Hypersonics, University of Queensland, Brisbane, Australia, Email: {r.gollan, p.jacobs}@uq.edu.au*

ABSTRACT

Numerical simulations of the re-entry of the International Space Station (ISS) are reported. By simplifying the large structure to the most significant modules, and using a combination of axisymmetric and 3D geometries, moderate sized simulations at various altitudes became possible. The simulations were run using the CFD software EILMER. Simulations for different altitudes and variations of the ISS geometry were performed investigating the heating amplification caused by shock impingement. The main result is that the shock impingement results in local surface heat flux magnifications of up to a factor of seven when compared to the heat flux resulting from a regular shock heating in free flight conditions. Additionally, using a typical shallow re-entry trajectory for the simulation points shows that the shock impingement location does not vary greatly in time. Therefore, future simulations of the re-entry break-up of the ISS can be significantly improved by integrating simple correlations to include shock impingement heating, most likely resulting in an earlier aerothermal material failure.

Keywords: re-entry; ISS; CFD.

1. INTRODUCTION

The upcoming re-entry of the International Space Station (ISS) represents the largest destructive entry in the history of space flight. This single event challenges the current understanding of re-entry aerothermodynamics for spacecraft break-up and debris trajectory analyses. The only other comparable object to enter the Earth's atmosphere was the Mir vehicle in 2001, however, at 19 m × 30 m × 30 m Mir was also considerably smaller than the ISS. The controlled destructive re-entry of a vehicle requires careful planning to ensure that there is minimal danger of parts surviving the re-entry and causing damage or loss of life on the ground. This is done by controlling the re-entry such that any surviving components land in a sparsely populated area, commonly the 'South Pacific Ocean Uninhabited Area' (SPOUA). How-

ever, the ability to plan re-entries in this fashion requires advanced, accurate models of the vehicle break-up and component trajectories.

Most destructive entries involve spacecraft with comparatively simple geometries, i.e. single part transports such as the Automated Transfer Vehicle (ATV) and Cygnus vehicles or satellites. When considering a multi-component structure, such as the ISS, the aerothermodynamic loading increases greatly in complexity due to the structure size and increased flow-structure interactions which occur, including shock impingement heating. The break-up modelling also increases in complexity, firstly due to the aerothermodynamic loads, and secondly due to the new failure modes in a large structure. In particular, the joints between the different components in a large structure provide likely failure points. Accurate modelling of the timing and mechanism of the break-up is important for modelling the trajectory of the different components, which is in turn crucial for assessing the size of the impact area.

This work is conducted within the ESA project 'ISS Atmospheric Break-up Analysis' (ISSABA) which is being undertaken by the High Enthalpy Flow Diagnostics group (HEFDiG) at the Institute of Space Systems (IRS) at the University of Stuttgart and Hyperschall Technologie Göttingen (HTG) with assistance from Institut de mécanique céleste et de calcul des éphémérides (IMCCE) and Astos Solutions. The objective of this project is to investigate the aerothermodynamic modelling of the ISS re-entry, the break-up modelling using the Spacecraft Atmospheric Re-Entry and Aerothermal Break-Up program (SCARAB) of HTG [6, 7], and provide a plan for a European airborne flight observation of the ISS re-entry. Flight observation missions represent the best possibility for verification and validation of the break-up model. IRS have been involved in every flight observation mission since Stardust, including ATV-1, Hayabusa, WT1190F, and Cygnus OA6 as well as being the science lead for the ATV-5 observation which was cancelled at the last minute due to an on-board power failure resulting in an earlier re-entry. Additionally, IRS is involved in investigating ground testing of joint strengths and other break-up mechanisms.

This paper is looking at the aerothermodynamic mod-

elling of the ISS, in particular looking at the localised heating caused by shock impingements. These local heating peaks are not relevant for single component vehicles and are hence not considered in most break-up modelling programs, however, they are of vital importance for a large structure re-entry. A prominent example of shock impingement heating is the X15 vehicle which had an unexpected structural failure due to the shock impingement heating on a supporting strut [9]. The data from X15 gives an indication of the heating effect which can occur, emphasising the need for a careful analysis of the shocks during a re-entry. The data sets developed in this work provide the basis for an extension of the SCARAB program for the implementation of variable heating loads to account for these effects.

2. AEROTHERMODYNAMIC MODELLING

Analysis of the open literature for the ISS End-of-Life (EoL) plan has shown that the most likely re-entry scenario is with the Russian segment entering first with at least one Progress module providing deceleration [8, 2]. Correspondingly, the geometry used for the modelling is based on the Russian segment. The region of interest is shown in Fig. 1 which includes the service module (SM), multipurpose laboratory module (MLM) and mini-research module (MRM).

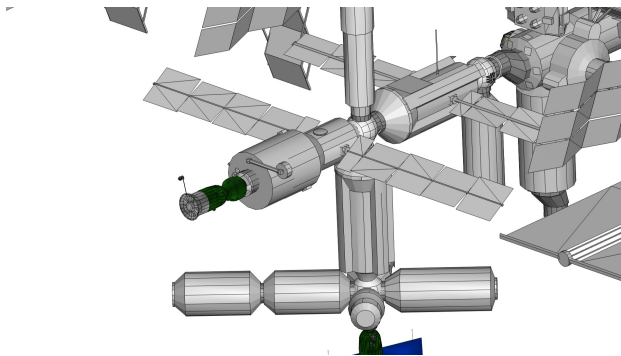


Figure 1. A zoomed view of the region of interest of the ISS for the re-entry modelling

A complete model of the ISS structure, which is physically very large at $75\text{ m} \times 100\text{ m}$, would require an unfeasible amount of detail and hence geometric simplifications are required for the modelling. Due to the size of the ISS, resolving every minor detail of the structure accurately in the CFD model would require billions of cells and a correspondingly large number of CPU hours. Although smaller structure details may cause some localised heating, the overall break-up scenario depends mainly on the local shock impingement heating. Therefore, the model is simplified to simple cylindrical geometries.

The resulting simplified geometry is shown in Fig. 2. Here the shock impinging on the vertical arm can be seen. The vertical arm is representative of any structure which

the shock may impinge upon. In this instance this would be the MLM as shown in Fig. 1. Within this paper when referring to the *arm* this means a 1 m radius cylinder upon which the shock impinges as shown. This impingement is the main point of interest for this work. Also seen in Fig. 2 is the separation of the flow domain into two sections. The upstream component of the model is modelled as a 2D axisymmetric component and the shock impingement section is modelled in 3D. The separation of the flow into these domains saves greatly on compute time allowing the primary shock to be modelled with higher resolution in the 2D domain.

Firstly the 2D simulation is run to completion. This computation includes the development of the here named primary shock over the front of the vehicle, which is in fact the Progress module. From this 2D flow field a *vertical* slice is then taken to provide the inflow for the 3D simulation. The coordinates of the flow field data are converted into 3D space and this data is then used as the 3D inflow data.

The aerothermodynamic modelling was conducted using CFD analysis assuming viscous flow of a chemically reacting, thermally perfect gas mixture of nitrogen and oxygen. A variety of flow conditions, representing different flight altitudes, around the altitudes of interest for break-up were analysed. The altitudes considered are based on previous re-entries, e.g. Skylab [4] and Mir [1]. The flow conditions for these altitudes were taken from the Cygnus OA6 trajectory, which was a shallow re-entry, similar to the trajectory that is anticipated for the ISS re-entry.

Table 1. Numerical simulation input parameters.

Altitude	80 km	70 km	60 km
Velocity	7668 m/s	7095 m/s	5980 m/s
Temperature	185.6 K	209.9 K	244.4 K
Pressure	1.0 Pa	5.5 Pa	24.0 Pa
Mass fraction, O ₂	0.22	0.22	0.22
Mass fraction, N ₂	0.78	0.78	0.78

In addition to varying the free-stream parameters, the distance of the vertical arm from the primary shock formation point was also varied. This allows inferences to be made about how the location of the structure being impinged upon will affect the resulting heat load. For this the baseline 70 km altitude condition was taken and the vertical arm simulated at 5 m, 16 m and 25 m from the primary shock. These locations can be seen in Fig. 3.

Also noticeable in Fig. 3 is that the full vertical arm is not shown. Due to the computational cost of the chemically reacting flow only the small regions around the main shock impingements were modelled. This allows the peak heating values from the impingement to be calculated whilst significantly reducing the overall computational cost.

The CFD analysis was undertaken using the multi-block

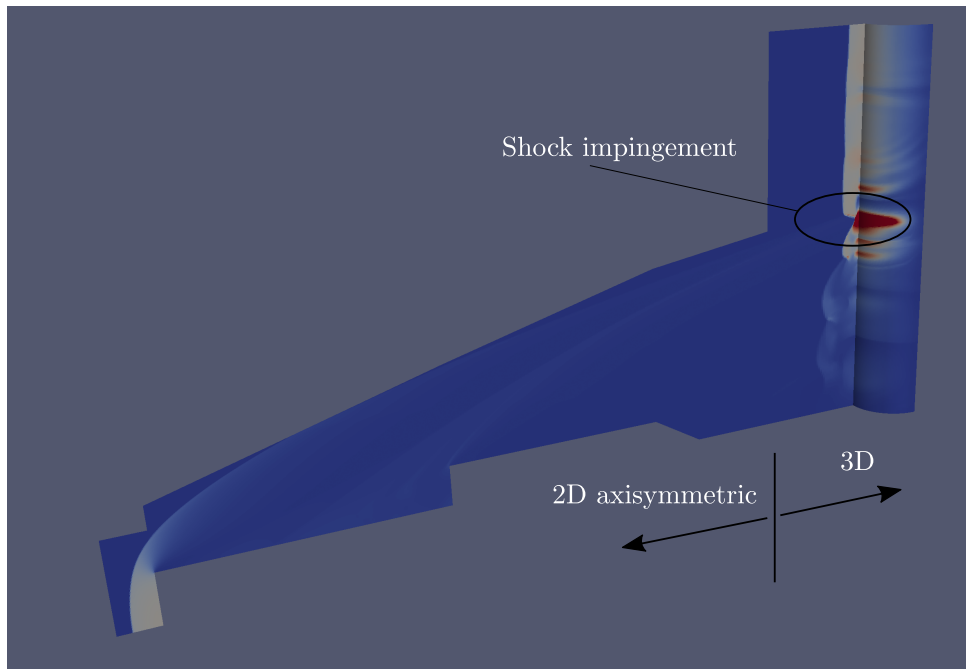


Figure 2. Simplified geometric flow model of the ISS

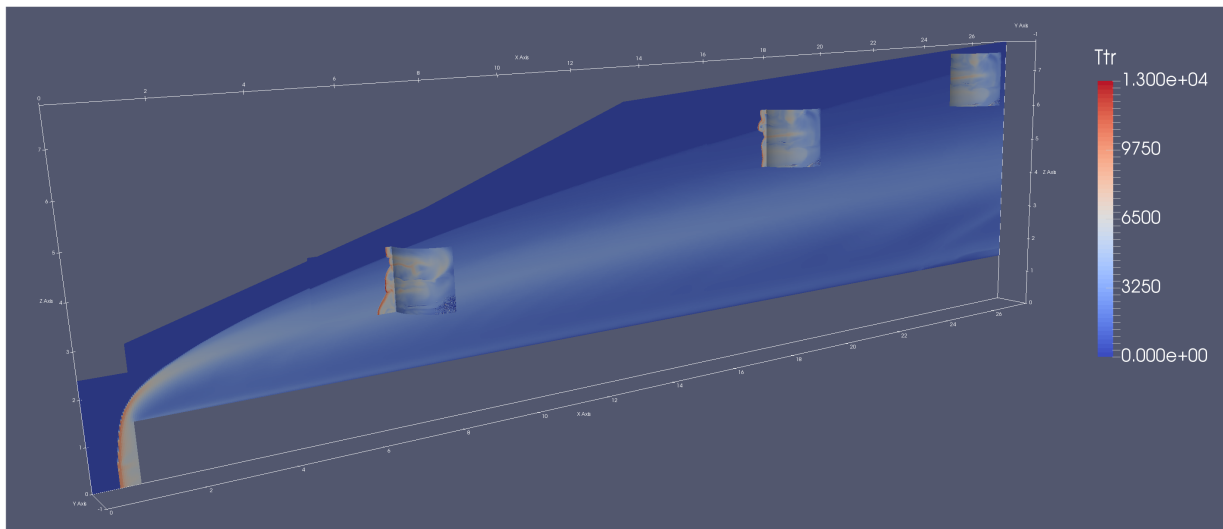


Figure 3. The inset 3D surfaces show the arms at different distances from primary shock

Navier-Stokes compressible flow solver EILMER [3], a code specialising in hypersonic, chemically reacting flows. EILMER is frequently used for re-entry simulations and has been validated and verified extensively against other numerical simulation, ground testing data and re-entry flight data. At the relevant conditions for the ISS re-entry, the thermochemistry will play an important role in the flow analysis, however, radiation and thermal non-equilibrium can be omitted from the analysis. A 5-species, 6 reaction chemistry scheme of Gupta et al. [5] was used.

3. NUMERICAL RESULTS

The numerical simulations were initially conducted using an ideal gas model to develop the geometries and gain an understanding of the flow behaviour expected. Figure 4 shows an example result of the heat flux levels computed on the vertical arm using ideal gas. In this image the 0 m distance around the arm refers to the stagnation line of the arm. The main feature which is evident is the location of the shock impingement where the heating is close to an order of magnitude higher than elsewhere.

Figure 5 shows the stagnation line heating from the sim-

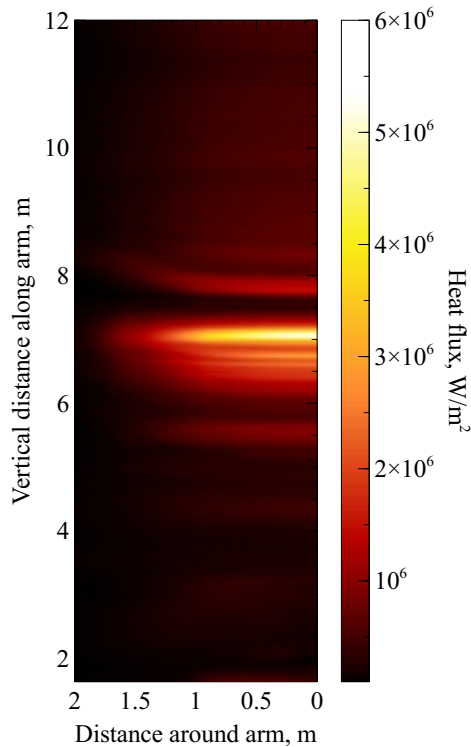


Figure 4. Cylinder surface heating

ulation in Fig. 4. This clearly shows the heating profile caused by the shock impingement. The minor ripples in the profile, and the small peak at $x = 2$ m, are the result of modelling simplifications resulting in non-physical artefacts in the profile, however, these are very small and do not affect the overall result. As this is an ideal gas model the heat flux loads cannot be considered to be realistic, however, the form of the heating profile should be fairly similar to that which occurs during a shock impingement computed with a reacting gas. This is important for the chemically reacting models as it allows a much smaller portion of the flow field to be modelled, that is just the shock impingement region, and with these approximations about the profiles, a heating load can be formulated for the break-up modelling.

The reacting gas simulations are conducted using the same two-stage process, however, the major difference to the ideal gas case is that the 3D simulation only encompassed the region of interest around the shock impingement as explained in Section 2. Figure 6 shows the stagnation line heating for the three different altitudes simulated. These results are computed with the arm at 16 m downstream from the primary shock. The free-stream heating levels onto the arm are also shown, this is the heating experienced by the arm in the region outside of the primary shock. The results are obtained from a set of 2D simulations over a cylinder to clarify the effect of the shock impingement on the heating load. The heating levels inside the shock are approximations also based on simplified computations.

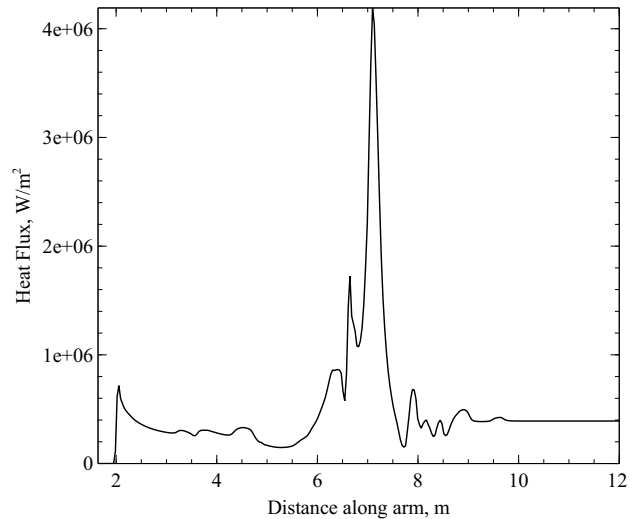


Figure 5. Stagnation line heat flux for an ideal gas at 70 km altitude

The results so far show that the shock impingement causes heat loads of up to seven times larger than the free-stream heating. This is a significant increase when considering the surface temperatures from which the material thermal failure will result. Although it is not immediately evident in Fig. 6, when considering the scale of the ISS, in the order of 100 m, the heating peaks from the shock impingement are very localised. Depending on the exact flow conditions, the high heating loads are spread over a 0.5 – 2 m distance.

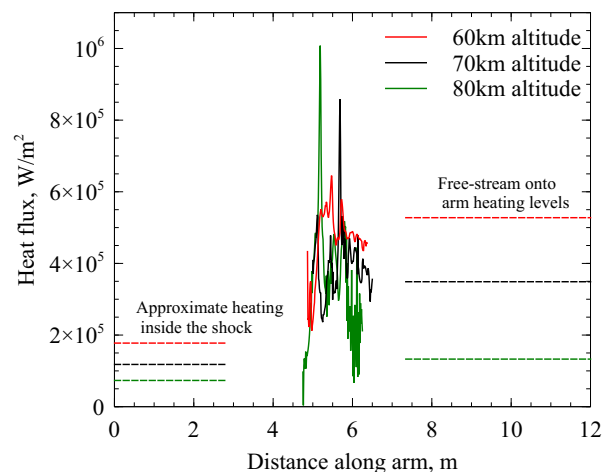


Figure 6. Heating profiles along stagnation lines at different altitudes

An interesting feature to notice is that the location of the peak heating along the arm does not change very much. With the slowing of the ISS it would be expected that the shock impingement would shift along the arm, however, the changing atmospheric conditions counter this ef-

fect and over the altitude range explored here the shock impingement location only shift by approximately 0.5 m (at a distance of 16 m from the primary shock). The other feature which can be seen in Fig. 6 is the broadening of the heating region. At lower altitudes, and hence higher densities, the heating region broadens distributing the heat into a larger section of the vehicle. This is another feature which is important for the break-up modelling input.

Although not of primary interest in this study, another effect of the shock impingement is a localised pressure increase. The pressure profile, shown in Fig. 7 for 70 km altitude at a distance of 16 m from the primary shock, is very similar to the heat flux profile with a very large localised peak. The pressure peak in itself would not be likely to cause any structural failures for break-up, however, localised pressure increases in addition to the heating peak may contribute to the localised failure of the structure. A higher pressure results in an additional mechanical load to the structure. Although no criteria for the mechanical failure of, for example, the nodes of the ISS are known, the higher pressure has to be considered as contributing to an acceleration of the failure.

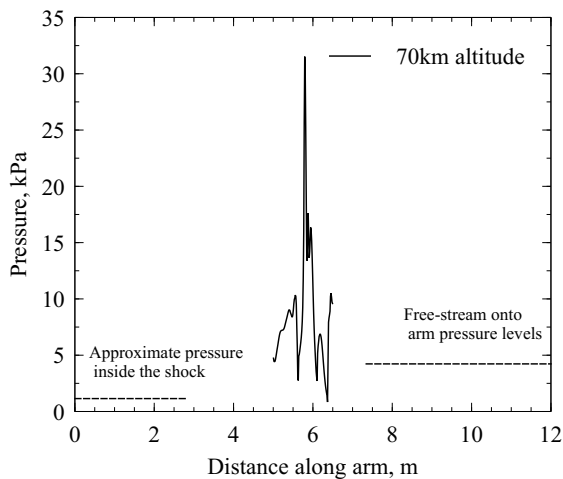


Figure 7. Pressure profile along stagnation line for the 70 km, 16 m from primary shock condition

The second part of this investigation is into the effect of the distance from the primary shock. Especially with an ISS sized structure there will be multiple shock impingement locations and therefore the effect of the downstream location of these impingements is also investigated. The results of simulations for 5 m, 16 m and 25 m downstream of the primary shock are shown in Fig. 8. The most noticeable effect is the shifting of the impingement along the vertical arm. This is expected based on the primary shock shape and can be clearly seen in Fig. 3.

The impingement point heat flux levels do not show a strong dependency on the distance from the primary shock. The peak heat flux levels reduce by approximately $1.0 - 1.5 \times 10^5 \text{ W/m}^2$ between each of the simulations,

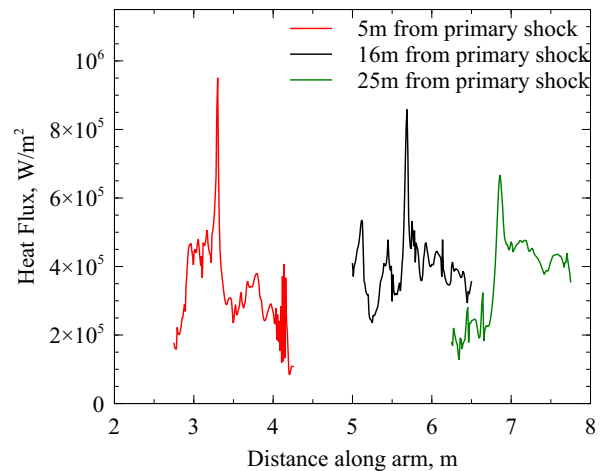


Figure 8. Heating at distances from primary shock

representing approximately 10 m downstream distance. This shows that even at a large distance behind the primary shock the impingement heating will still be significant. For the ISS this means there will be substantial impingement heating on the truss section. Additionally, although the locations further downstream have a lowered heating, this heating is dissipated over a larger region of the arm. This means that a larger area of the structure experiences the enhanced heating.

4. CONCLUSION

The upcoming End-of-Life of the ISS will be the largest ever destructive atmospheric re-entry of a space vehicle. This presents new challenges for the break-up modelling community, in particular considering the aerothermodynamic loads which will be experienced. This work has presented some initial numerical modelling of the ISS entry, in particular investigating the shock impingement phenomena. This is an effect which is generally not experienced by the geometrically simple re-entry objects such as the ATVs, Cygnus or other satellites, and has therefore not previously been considered during the break-up modelling.

A geometrically simplified model of the re-entering ISS forebody has been constructed and the flow field was analysed over a variety of flow conditions. The numerical modelling was conducted using the EILMER CFD package. Simulations were conducted at 80 km, 70 km and 60 km altitudes, where the flow conditions were taken from the Cygnus OA6 re-entry trajectory. Additionally, shock impingements at various distances downstream of the primary shock were investigated.

Heat flux levels from a shock impingement on a vertical arm result in localised heat flux levels of up to seven

times larger than the free-stream heat flux levels. The elevated heat flux levels are localised to a 1–2 m region. In the simulations conducted here the location of the impingement did not change significantly with altitude, the decreasing flight velocity was compensated for by the increasing pressure resulting in a relatively stable shock impingement location. Additional to the heat flux peak, the shock impingement also causes a pressure peak at the same location.

The distance downstream of the primary shock did not greatly affect the heat flux peak from the shock impingement. This means that any component of the ISS upon which the primary shock impinges will experience a locally significantly elevated heat flux. The location of the impingement is the result of the structural geometry.

The results of these simulations have highlighted the importance of considering the shock impingements which will occur during the re-entry of a large structure. Additionally heat flux profile data has been provided for break-up modelling of ISS re-entry.

ACKNOWLEDGEMENTS

This work is supported by the ESA project 'ISS Atmospheric Break-up Analysis', 4000116300/15/D/SR.

REFERENCES

1. Christy, R. (2001). Mir re-entry. <http://www.zarya.info/Tracking/Mir/Mir-Re-entry2.php>.
2. Duncan, G. W. (2014). International space station end-of-life probabilistic risk assessment. In *Probabilistic Safety Assessment and Management*.
3. Gollan, R. J. and Jacobs, P. A. (2013). About the formulation, verification and validation of the hypersonic flow solver eilmer. *International Journal for Numerical Methods in Fluids*, 73:19–57.
4. Gray, C. (2016). Iss end of life strategy and contingency action plan. Technical Report SSP 51066, NASA.
5. Gupta, R. N., Lee, K.-P., Thomson, R. A., and Yos, J. M. (1990). A review of reaction rates and transport properties for an 11-species air model for chemical and thermal nonequilibrium calculations to 30000 k. Technical Report TM 85820, NASA.
6. Koppenwallner, G., Fritsche, B., Lips, T., and Klinkrad, H. (2005). Scarab - a multi-disciplinary code for destruction analysis of spacecraft during re-entry. In *5th European Symposium on Aerothermodynamics for Space Vehicles*. ESA.
7. Lips, T., Fritsche, B., Koppenwallner, G., and Klinkrad, H. (2004). Spacecraft destruction during re-entry latest results and development of the scarab software system. *Advances in Space Research*, 34(5):1055–1060.
8. Suffredini, M. T. (2010). ISS end-of-life disposal plan. Technical report, NASA.
9. Watts, J. D. (1968). Flight experience with shock impingement and interference heating on the x-15-2 research airplane. Technical Report NASA TM X-1669, NASA.